Agricultural and Forest Meteorology 226–227 (2016) 174–185

Contents lists available at ScienceDirect

Agricultural and Forest Meteorology

journal homepage: www.elsevier.com/locate/agrformet

Evaluation of the Community Land Model simulated carbon and water fluxes against observations over ChinaFLUX sites☆

Li Zhang[a], Jiafu Mao[b], Xiaoying Shi[b], Daniel Ricciuto[b], Honglin He[a], Peter Thornton[b], Guirui Yu[a,*], Pan Li[c], Min Liu[d], Xiaoli Ren[a], Shijie Han[e], Yingnian Li[f], Junhua Yan[g], Yanbin Hao[h], Huimin Wang[a]

[a] Key Laboratory of Ecosystem Network Observation and Modeling, Institute of Geographic Sciences and Natural Resources Research, Chinese Academy of Sciences, Beijing 100101, China
[b] Environmental Sciences Division and Climate Change Science Institute, Oak Ridge National Laboratory, Oak Ridge, TN, USA
[c] Institute of Geochemistry, Chinese Academy of Sciences, Guiyang 550081, China
[d] Shanghai Key Laboratory for Urban Ecology and Sustainability, East China Normal University, Shanghai 200062, China
[e] Institute of Applied Ecology, Chinese Academy of Sciences, Shenyang 110016, China
[f] Northwest Institute of Plateau Biology, Chinese Academy of Sciences, Xining 810001, China
[g] South China Botanical Garden, Chinese Academy of Sciences, Guangzhou 510650, China
[h] University of Chinese Academy of Sciences, Beijing 100049,China

ARTICLE INFO

Article history:
Received 6 September 2015
Received in revised form 13 April 2016
Accepted 22 May 2016

Keywords:
Community land model
ChinaFLUX
Eddy covariance
Carbon flux

ABSTRACT

The Community Land Model (CLM) is an advanced process-based land surface model that simulates carbon, nitrogen, water vapor and energy exchanges between terrestrial ecosystems and the atmosphere at various spatial and temporal scales. We use observed carbon and water fluxes from five representative Chinese Terrestrial Ecosystem Flux Research Network (ChinaFLUX) eddy covariance tower sites to systematically evaluate the new version CLM4.5 and old version CLM4.0, and to generate insights that may inform future model developments. CLM4.5 underestimates the annual carbon sink at three forest sites and one alpine grassland site but overestimates the carbon sink of a semi-arid grassland site. The annual carbon sink underestimation for the deciduous-dominated forest site results from underestimated daytime carbon sequestration during summer and overestimated nighttime carbon emission during spring and autumn. Compared to CLM4.0, the bias of annual gross primary production (GPP) is reduced by 24% and 28% in CLM4.5 at two subtropical forest sites. However, CLM4.5 still presents a large positive bias in annual GPP. The improvement in net ecosystem exchange (NEE) is limited, although soil respiration bias decreases by 16%–43% at three forest sites. CLM4.5 simulates lower soil water content in the dry season than CLM4.0 at two grassland sites. Drier soils produce a significant drop in the leaf area index and in GPP and an increase in respiration for CLM4.5. The new fire parameterization approach in CLM4.5 causes excessive burning at the Changbaishan forest site, resulting in an unexpected underestimation of NEE, vegetation carbon, and soil organic carbon by 46%, 95%, and 87%, respectively. Overall, our study reveals significant improvements achieved by CLM4.5 compared to CLM4.0, and suggests further developments on the parameterization of seasonal GPP and respiration, which will require a more effective representation of seasonal water conditions and the partitioning of net radiation between sensible and heat fluxes.

* Corresponding author.
E-mail address: yugr@igsnrr.ac.cn (G. Yu).

http://dx.doi.org/10.1016/j.agrformet.2016.05.018
0168-1923/

1. Introduction

Reliable estimations of carbon and water vapor exchanges between terrestrial ecosystems and the atmosphere are essential to predicting the global terrestrial carbon cycle and its feedback to anthropogenic climate change. Although dozens of process-based terrestrial biosphere models have been developed and applied in assessing the past, present, and future global carbon cycle, considerable uncertainties still remain in the simulation and analysis of terrestrial ecosystem carbon fluxes from regional (Forster et al., 2013; Jung, 2007b; Morales et al., 2005; Piao et al., 2011; Wenzel et al., 2014) to global scales (Cramer et al., 2001; Friedlingstein et al., 2003; Friedlingstein et al., 2014; Piao et al., 2013; Sitch et al., 2008). Several model-data intercomparison studies have been conducted in recent years to evaluate the performance of various terrestrial ecosystem models in simulating carbon and water fluxes based on eddy covariance flux observations in North America (Huntzinger et al., 2012; Jung, 2007a; Raczka et al., 2013; Schaefer et al., 2012; Schwalm et al., 2010), Europe (Balzarolo et al., 2014), and East Asia (Ichii et al., 2013). Data from the Free-air CO_2 enrichment (FACE) experiments at Duke Forest (Durham, North Carolina, USA) and Oak Ridge National Laboratory (Oak Ridge, Tennessee, USA), and nitrogen addition experiments at the Duke Forest site, have also been used to assess the ability of terrestrial ecosystem models to predict water, carbon, and nitrogen cycles at ambient and elevated CO_2 concentrations (De Kauwe et al., 2013; De Kauwe et al., 2014; Walker et al., 2014; Zaehle et al., 2014) and nitrogen limitations (Thomas et al., 2013). However, none of these models accurately simulates water and carbon fluxes and ecosystem responses to long-term elevated atmospheric CO_2 and nitrogen additions at all selected sites. Models have performed poorly in terms of canopy phenology predictions, responses to drought during the growing season, and nutrient limitations, due to an insufficient understanding of underlying processes or an inaccurate representation of biological processes and parameters. Additional knowledge of processes related to terrestrial ecosystems and their interactions within the Earth system (Bonan, 2014) and more detailed evaluations of individual models are of vital importance to model development.

Of the 11 Earth system models involved in the World Climate Research Programme's phase 5 of the Coupled Model Intercomparison Project (CMIP5), which generated climate projections for the Fifth Assessment Report of the Intergovernmental Panel for Climate Change (IPCC AR5), only two models (the Community Earth System Model (CESM) and Norwegian Earth System Model) include a dynamic terrestrial nitrogen cycle (Friedlingstein et al., 2014). Both of these use the Community Land Model (CLM) as the land component. The CLM is a state-of-the-art land surface model for simulating biogeophysical and biogeochemical processes in the atmosphere-vegetation-soil continuum (Oleson et al., 2013). CLM has been evaluated for different soil and vegetation types across various scales for many variables including albedo (Wang et al., 2004), Leaf Area Index (LAI) (Kim and Wang, 2005; Lawrence and Chase, 2007), streamflow, surface runoff, soil moisture, river flow (Boisserie et al., 2006; PaiMazumder et al., 2008; Qian et al., 2006; Shi et al., 2011), snow cover fractions (Lawrence et al., 2011; Niu and Yang, 2007), discharge (Lawrence et al., 2011; Swenson et al., 2012), gross primary production (GPP), and evapotranspiration (ET) (Bonan et al., 2011; Mao et al., 2015, 2012; Shi et al., 2013). At the site scale, data from 15 FLUXNET tower sites were used to identify the deficiencies of CLM3.0 and development of CLM3.5 in soil hydrology (Stockli et al., 2008). Some case studies have also been conducted to validate energy and carbon budget at flux tower sites (Lee et al., 2013; Li et al., 2011; Wang et al., 2008) and streamflow using earlier versions of the CLM (Niu et al., 2005).

Previous evaluations of CLM have primarily focused on terrestrial ecosystems in the western hemisphere. Few studies have evaluated the performance of CLM based on site-level observations of the intense East Asian monsoon region, including unique terrestrial ecosystems in Qinghai-Tibet Plateau with low atmospheric CO_2 and strong solar radiation, and subtropical zone where the forest acts as a high carbon sink (Yu et al., 2014). The Chinese Terrestrial Ecosystem Flux Research Network (ChinaFLUX) obtains data on net ecosystem exchanges of CO_2, H_2O, and heat flux in typical Chinese ecosystems (Yu et al., 2006) and provides valuable data for the evaluation and development of terrestrial ecosystem models (He et al., 2014; He et al., 2013; Huang et al., 2007; Ichii et al., 2013; Ju et al., 2010; Ren et al., 2013; Tao et al., 2007; Yan et al., 2009; Zhang et al., 2010) in China. The objectives of this study are to evaluate two versions of CLM (CLM4.0 and CLM4.5) in simulating carbon and water fluxes based on measurements collected at five representative ChinaFLUX sites, to investigate major model errors and sources of uncertainty and to propose possible improvements to potential applications of CLM in estimating terrestrial ecosystem carbon cycle dynamics across continental China.

2. Methods

2.1. Site description

The data used in this study were obtained from five ChinaFLUX sites (Fig. S1): the Changbaishan temperate broad-leaved Korean pine mixed forest (CBS), Qianyanzhou subtropical coniferous plantation (QYZ), Dinghushan subtropical evergreen coniferous and broad-leaved mixed forest (DHS), Inner Mongolia temperate steppe (NMG), and Haibei alpine shrub-meadow (HBG). Mean annual temperatures were 3.6 °C, 17.9 °C, 20.9 °C, 0.4 °C and −1.7 °C for the CBS, QYZ, DHS, NMG, and HBG, respectively. Average annual precipitation values for 2003–2008 were 713, 1542, 1956, 351, and 580 mm, respectively. The Changbaishan temperate mixed forest is an old growth forest with a stand age of over 200 years situated in Northeastern China. The NMG and HBG are two typical grassland sites located within the Xilin River Basin of northern China and Qinghai-Tibet Plateau, respectively. The QYZ and DHS are two subtropical forests in southern China. Vegetation was converted from the original evergreen broadleaf forest to grassland as a result of human activities occurring prior the 1980s in the QYZ. Following the establishment of the QYZ station in 1983, coniferous trees were planted in the area, and they have not been disturbed since then (Huang et al., 2007). The DHS mixed forest is a succession community where evergreen broadleaf species have gradually invaded after *pinus massoniana* planting in the 1950s (Zhang et al., 2006a). Brief descriptions of the sites' characteristics are presented in Table 1. Detailed descriptions are available in Zhang et al. (2006b) and Yu et al. (2008) for the CBS, QYZ, and DHS; in Zhaoet al. (2006) and Hu et al. (2008) for the HBG; and in Hao et al. (2006) and Fu et al. (2006) for the NMG.

2.2. Data

2.2.1. Forcing data

Both CLM4.0 and CLM4.5 require downwelling long-wave radiation ($W\,m^{-2}$), downwelling short-wave radiation ($W\,m^{-2}$), air temperature (K), precipitation ($mm\,s^{-1}$), relative humidity (%), surface pressure (Pa), and wind speed ($m\,s^{-1}$) data to conduct off-line simulations. Observed meteorological data at five sites were gap-filled at half-hourly time steps following methods used for North American Carbon Cycle interim synthesis (Schwalm et al., 2010). Missing meteorological data values were filled using observations made from a meteorological observation station located at the

Table 1
Site characteristics of five ChinaFLUX sites.

Site name	CBS	QYZ	DHS	NMG	HBG
Longitude (E)	128.096	115.058	112.57	116.67	101.33
Latitude (N)	42.403	26.741	23.17	43.55	37.67
Elevation (m)	738	102	300	1189	3327
Tower height (m)	61.8	45	36	2.2	2.2
Mean annual temperature [a] (°C)	3.6	17.9	21.0	0.4	−1.7
Annual precipitation [a] (mm)	695	1485	1956	351	580
Plant functional type	BDF (75%) NEF (25%)	NEF(100%)	BEF(90%)NEF(10%)	C3G(90%)C4G(10%)	C3G(55%)BDS(40%)C4G(5%)
Land use type	Forest	Forest	Forest	Grassland	Grassland
Soil type	Upland dark brown forest soil	Typical red soil	Lateritic red soil	Chernozem soil	Alpine meadow soil
Years	2003–2008	2004–2008	2003–2008	2004–2005	2004–2007

BDF: broad-leaf deciduous forest; NEF: needle-leaf evergreen forest; BEF: broad-leaf evergreen forest; C3G: C3 grassland; C4G: C4 grassland; BDS: broad-leaf deciduous shrub.

same site within the Chinese Ecosystem Research Network (CERN) dataset (http://www.cerndata.ac.cn). In the absence of station data, a seven-day running mean diurnal cycle was used. In addition to meteorological data, soil texture, plant functional type and land use land cover change data were also collected at five flux sites as model inputs.

2.2.2. Eddy covariance flux measurements and data processing

Half-hourly averaged measurements of net ecosystem exchange (NEE) of CO_2, sensible (H) and latent heat (LE) fluxes used in model evaluations were measured in five ecosystems using open-path eddy covariance techniques. Detailed information on the instruments and data quality evaluation technique is available in Yu et al. (2006). Outlier data were rejected, and unreasonable nighttime values were excluded using friction velocity thresholds (Yu et al., 2008; Zhang et al., 2006b). Gaps in half-hourly CO_2 and water flux data were filled using a nonlinear regression algorithm (Falge et al., 2001). GPP and ecosystem respiration (RE) were estimated from half-hourly NEE following Zhang et al. (2006b) and Yu et al. (2008).

2.2.3. Soil respiration data measured using the static chamber technique

Soil respiration was measured once or twice per week during the growing season and once or twice per month in the winter using static chamber-gas chromatograph techniques at three forest sites and at the Haibei grassland site. During each measurement procedure, six samples were collected from 9:00 to 11:30 AM. All samples were analyzed in the laboratory using a HP4890D Gas Chromatographer on the sampling days. The number of overall sampling days was 135 for the CBS, 110 for the DHS, 114 for the QYZ, and 65 for the HBG. The soil respiration measurement method is described in detail in Zhang et al. (2006a) and Zheng et al. (2009). We estimated daily soil respiration by assuming a constant rate for each sample day.

2.3. Model

The carbon-nitrogen version of CLM4.0 (CLM-CN) was the first to explicitly characterize the effects of nitrogen on terrestrial ecosystem dynamics and feedback to the climate in an Earth System Model (Bonan et al., 2012; Shi et al., 2013; Thornton et al., 2009; Thornton et al., 2007). CLM4.0 was found to present notable biases in simulated GPP, ET, LAI, and soil carbon stocks (Oleson et al., 2013). Due to these known biases, corresponding modifications were implemented to the subsequent version of CLM (CLM4.5) by incorporating recent scientific advances in land-surface process modeling, including representations of photosynthesis (Bonan et al., 2011; Sun et al., 2012), hydrological processes (Swenson et al., 2012; Swenson and Lawrence, 2012), fire (Li et al., 2012, 2013), and soil biogeochemical processes (Koven et al., 2013). Detailed descriptions of these modifications for CLM4.5 can be found in Oleson et al. (2013).

We conducted CLM4.0 and CLM4.5 simulations at the five ChinaFLUX sites using the structure of the Point Version of CLM (PTCLM, described in Oleson et al., 2013), which performs simulations for a single model grid cell using site-measured meteorology features, soil characteristics, plant functional type distributions and land-use histories. We assumed that there was no disturbance at the CBS, NMG, and HBG sites, but imposed land cover changes at the QYZ and DHS sites according to the land-use histories of each site. Here we used the CLM-CN (Community Land Model with prognostic Carbon and Nitrogen) option for CLM4.0 and CLM4.5. Further information on the structure and spin-up methodologies of the PTCLM are given in Oleson et al. (2013).

3. Results

Comparisons between the modeled and observed NEE, H, and LE are shown in Fig. 1 (Taylor diagram) and Table 2 (R and RMSE). Fig. 2 shows the mean bias errors of annual GPP, RE, NEE, H, and LE and comparisons of monthly mean carbon and water fluxes for 2003–2008 between models and eddy flux observations.

3.1. Net ecosystem exchange of CO_2

The correlation coefficients of hourly NEE between the model and observations are similar between the two model versions at the five ChinaFLUX sites. Hourly NEE shows a higher correlation (R) at three forest sites (0.87–0.89) than at two grassland sites (0.50–0.68). Compared to CLM4.0, CLM4.5 shows a lower RMSE of hourly NEE at two subtropical sites (QYZ and DHS) but presents almost the same RMSE at the other three sites. In CLM4.5, the RMSE for hourly NEE decreases from 0.17 to 0.14 g C m^{-2} at QYZ and from 0.21 to 0.12 g C m^{-2} at DHS compared to CLM4.0.

The performance of CLM4.0 and CLM4.5 in simulating monthly NEE is different than that for hourly NEE. There is a slight improvement in modeled monthly NEE at CBS and QYZ for CLM4.5 compared to CLM4.0. R for monthly NEE increases from 0.70 to 0.78 at CBS and from 0.70 to 0.77 at QYZ. The RMSE of monthly NEE decreases from 37.61 to 34.01 g C m^{-2} at CBS and from 31.19 to 26.53 g C m^{-2} at QYZ. However, R decreases significantly from 0.44 to 0.03 and RMSE increases from 28.99 to 42.34 g C m^{-2} for monthly NEE at HBG. At the DHS site, R for monthly NEE shows a slight decrease, but RMSE decreases by 16.5%. At NMG, R remains at 0.47, but RMSE decreases from 20.05 to 18.97 g C m^{-2} for monthly NEE.

3.2. Sensible heat flux

CLM4.5 performs almost the same as CLM4.0 in modeling hourly sensible head flux (H). Both the R and RMSE of hourly H show con-

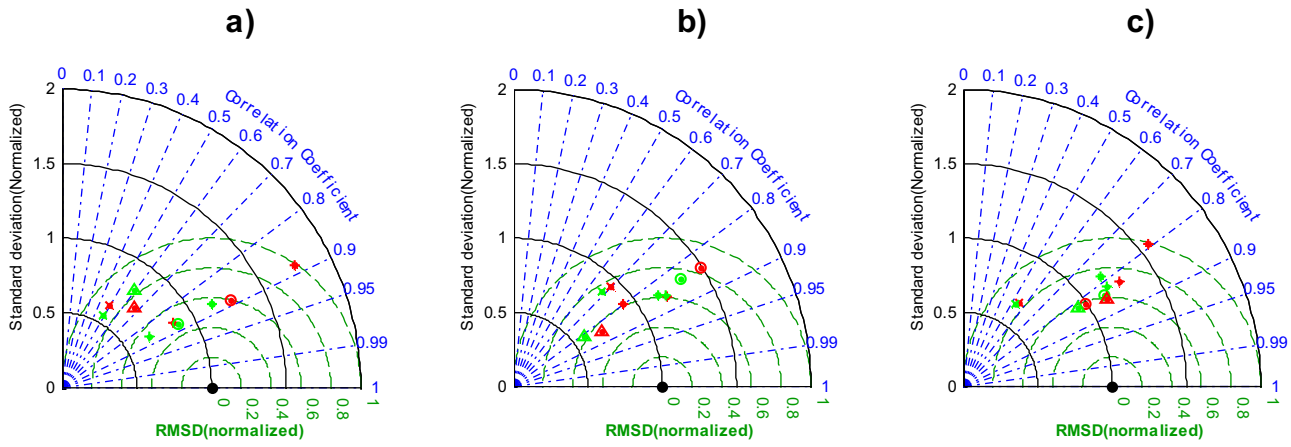

Fig. 1. Performance of CLM4.0 (red symbols) and CLM4.5 (green symbols) compared to observations (black solid points) made at five ChinaFLUX sites. Statistics shown in the Taylor diagram are derived from hourly simulated and observed NEE (a), H (b), and LE (c) fluxes. Legend: CBS: plus sign; QYZ: circle; DHS: asterisk; HBG: triangle; NMG: cross (for interpretation of the references to color in this figure legend, the reader is referred to the web version of this article.)

Table 2
Performance of simulated NEE, H, and LE from two versions (CLM4.0 and CLM4.5): R and RMSE (in brackets) are diagnosed on hourly and monthly timescales.

	NEE		H		LE	
Site	CLM4.0	CLM4.5	CLM4.0	CLM4.5	CLM4.0	CLM4.5
Hourly						
CBS	0.86(0.13)	0.87(0.13)	0.86(52.85)	0.86(54.21)	0.83(42.17)	0.82(39.90)
QYZ	0.89(0.17)	0.88(0.14)	0.92(49.30)	0.92(39.41)	0.86(45.71)	0.87(47.93)
DHS	0.89(0.21)	0.87(0.12)	0.80(45.24)	0.85(45.22)	0.79(72.75)	0.78(53.40)
HBG	0.68(0.10)	0.60(0.11)	0.85(52.24)	0.81(59.58)	0.85(45.27)	0.82(44.65)
NMG	0.50(0.05)	0.50(0.05)	0.70(70.20)	0.68(70.22)	0.55(41.25)	0.53(41.86)
Monthly						
CBS	0.70(37.61)	0.78(34.01)	0.44(18.95)	0.33(20.63)	0.97(9.03)	0.96(8.73)
QYZ	0.70(31.19)	0.77(26.53)	0.71(20.12)	0.69(14.19)	0.90(14.13)	0.87(17.23)
DHS	0.32(36.72)	0.25(33.63)	0.28(12.35)	0.45(11.78)	0.90(24.13)	0.90(13.18)
HBG	0.44(28.99)	0.03(42.34)	0.76(12.71)	0.68(14.73)	0.90(17.86)	0.86(19.21)
NMG	0.47(20.05)	0.47(18.97)	0.50(29.13)	0.50(28.38)	0.74(15.03)	0.72(15.60)

stant values or slight changes at the five sites (except for the QYZ, which shows a decreased RMSE in CLM4.5). The two CLM models exhibit poorer performance for monthly H than that for hourly H. R for monthly H ranges from 0.33 to 0.76, which is lower than that for hourly H (ranging from 0.68 to 0.86) (Table 2). The two models do not capture the second H peak in the autumn at HBG (Fig. 2i), as monthly averaged values of hourly H at 11–18 LST are underestimated by 42.4, 76.7, 70.4, and 62.3 W m^{-2} in September, October, November, and December at HBG (Fig. 3d).

Monthly H modeled by CLM4.0 and CLM4.5 had similar seasonal patterns at the CBS, QYZ, HBG, and NMG sites but major differences at the DHS site (Fig. 2i). Both models overestimated monthly H by 16.5 and 18.0 W m^{-2} on average at CBS and by 17.6 and 11.7 W m^{-2} at QYZ. At DHS, CLM4.0 presents a lower H while CLM4.5 presents excess H in most months (Fig. 2i). The monthly H simulation at DHS was improved in CLM4.5, presenting lower RMSE and higher R values (Table 2). The contribution to H from bare soil remained low at the three forest sites except during the non-growing season at CBS, while the term of H from vegetation was even higher than the observed total H by average values of 10.7 W m^{-2} in CLM4.0 and 11.7 W m^{-2} in CLM4.5 at CBS, 18.0 W m^{-2} in CLM4.0 and 11.7 W m^{-2} in CLM4.5 at QYZ, and 8.1 W m^{-2} in CLM4.5 at DHS.

3.3. Latent heat flux

CLM4.0 and CLM4.5 show similar behaviors in modeling hourly and monthly LE (Table 2). Changes in R and RMSE are very small except for the DHS site, where RMSE decreases from 72.75 W m^{-2} to 53.40 W m^{-2} for hourly LE and from 24.13 W m^{-2} to 13.18 W m^{-2} for monthly LE. Overall, the R for monthly LE is much higher than that for monthly H. This result suggests that the two models better reproduce the timing for LE than that for H. However, the models overestimate LE for the summer of 2005 at QYZ by 43–68 W m^{-2} and overestimate by 15 W m^{-2} on average for the summers of 2003–2008 at DHS (Figs. 2e and j). Although CLM4.5 improved GPP estimations at QYZ and DHS, it shows higher canopy transpiration and water storage than CLM4.0 by 19.3% and 13.8% at QYZ and higher ground evaporation and water storage by 80.9% and 20.8% at DHS, respectively. Furthermore, the observed Bowen ratio is 0.35 ± 0.06 at QYZ (Tang et al., 2014) while simulated values are 0.70 ± 0.04 for CLM4.0 and 0.53 ± 0.09 for CLM4.5. The better estimation in Bowen ratio indicates that CLM4.5 improves the partitioning of net radiation between latent and sensible heat fluxes, but still has a large bias.

3.4. Subtropical forest

CLM4.0 shows a significant excess GPP at the two subtropical forest sites (QYZ and DHS) (Fig. 2a). The modifications in photosynthesis in CLM4.5 decrease the mean bias in annual GPP by 70% and 54% at the two sites, respectively. Taking DHS as an example, the modeled solar radiation absorbed by vegetation is reduced by 4% due to a change in the solution for radiative transfer used in CLM4.5 compared to CLM4.0. The improvement in calculating leaf photosynthesis and stomatal conductance results in a 6% and 24% decrease for modeled shaded and sunlit leaf photosynthesis, respectively. Overall modifications in photosynthesis processes (including radiative transfer, leaf photosynthesis and stomatal con-

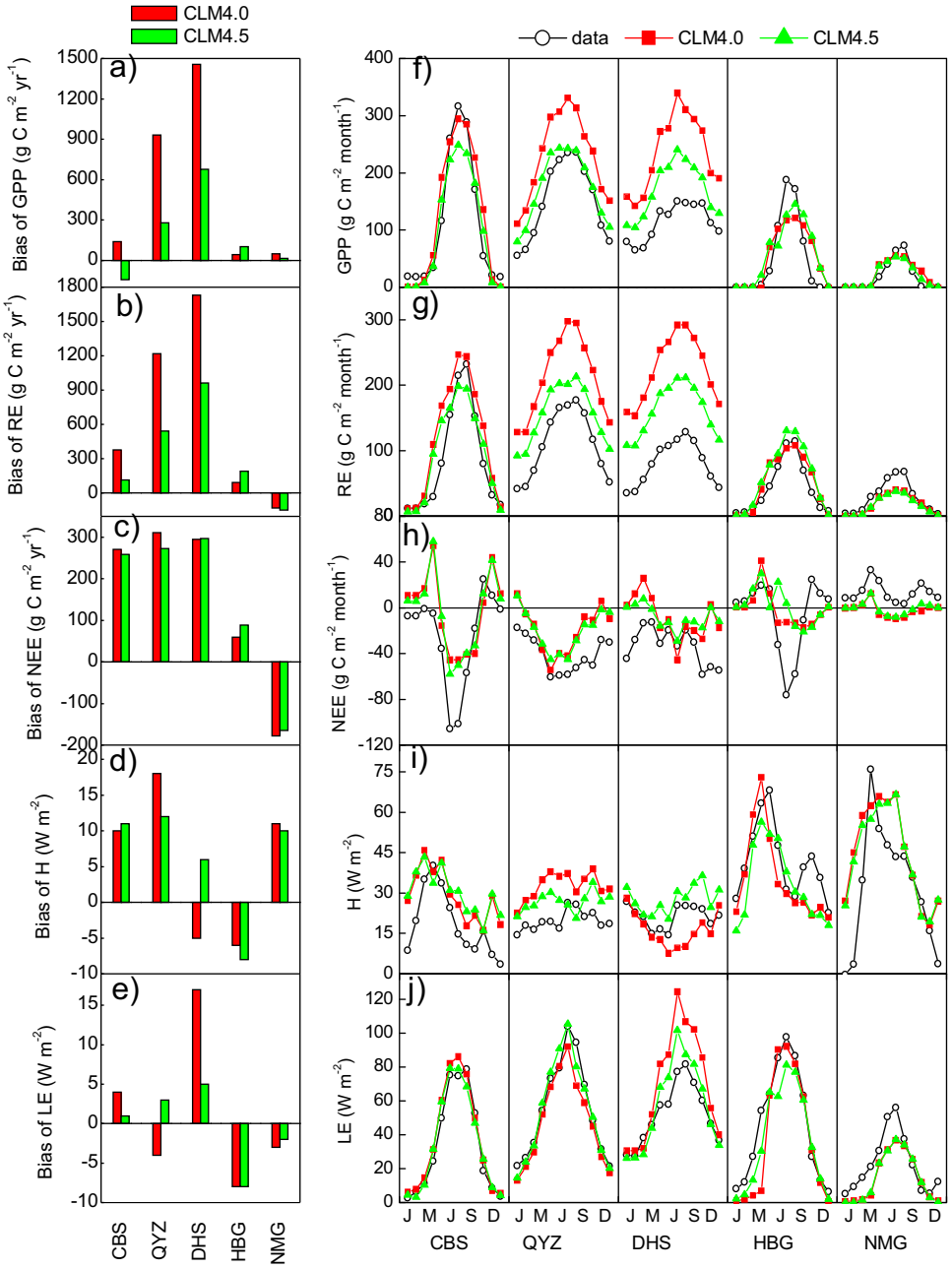

Fig. 2. Mean bias errors of annual GPP (a), RE (b), NEE (c), H, (d), and LE (e) and mean monthly GPP (f), RE (g), NEE (h), H (i), and LE (j) at the CBS, QYZ, DHS, HBG, and NMG sites from 2003 to 2008.

ductance, and canopy integration) in CLM4.5 produced reductions of 25% and 31% for C fixation from sunlit and shaded canopies, respectively. Compared to the observed LAI from the CERN dataset, modeled LAI is overestimated by 15% and 12% at QYZ and DHS, respectively, and this may have partly caused the excess GPP found in CLM4.5.

The new photosynthesis scheme in CLM4.5 contributes to lower vegetation carbon, which is reduced by 18% and 28% at QYZ and DHS. Accordingly, autotrophic respiration is reduced by 27% and 30%, contributing 88% and 73% to the reduction of annual RE bias (542 and 964 g C $m^{-2}yr^{-1}$ or 55% and 44%) at the two sites, respectively. Despite the considerable decline in GPP and RE biases at the two subtropical sites, improvements in NEE are limited, as annual GPP and RE were reduced simultaneously. Annual RE is overestimated more than annual GPP (Fig. 2b). The annual RE bias in CLM4.5 is 1.9 and 1.4 times that of annual GPP bias at QYZ and DHS, respectively. Additional comparisons between observed and simulated soil respiration (SR) shown in Fig. 4 illustrate that CLM4.5 overestimated daily SR with a bias of 1.61 g C m^{-2} d^{-1} and 1.00 g C m^{-2} d^{-1}, although RMSE for SR were reduced by 15.8% and 43.5% at the QYZ and DHS, respectively (Table 3). The simulated SR components provide insight into overestimations of respiration. The most significant contributor to total CO_2 efflux from the soil is found to

Table 3
Performance of simulated daily soil respiration in two versions (CLM4.0 and CLM4.5): R and RMSE (in brackets).

Site	CLM4.0	CLM4.5
CBS	0.70(2.19)	0.69(1.69)
QYZ	0.75(1.84)	0.77(1.55)
DHS	0.81(2.00)	0.82(1.13)
HBG	0.59(1.04)	0.66(1.05)

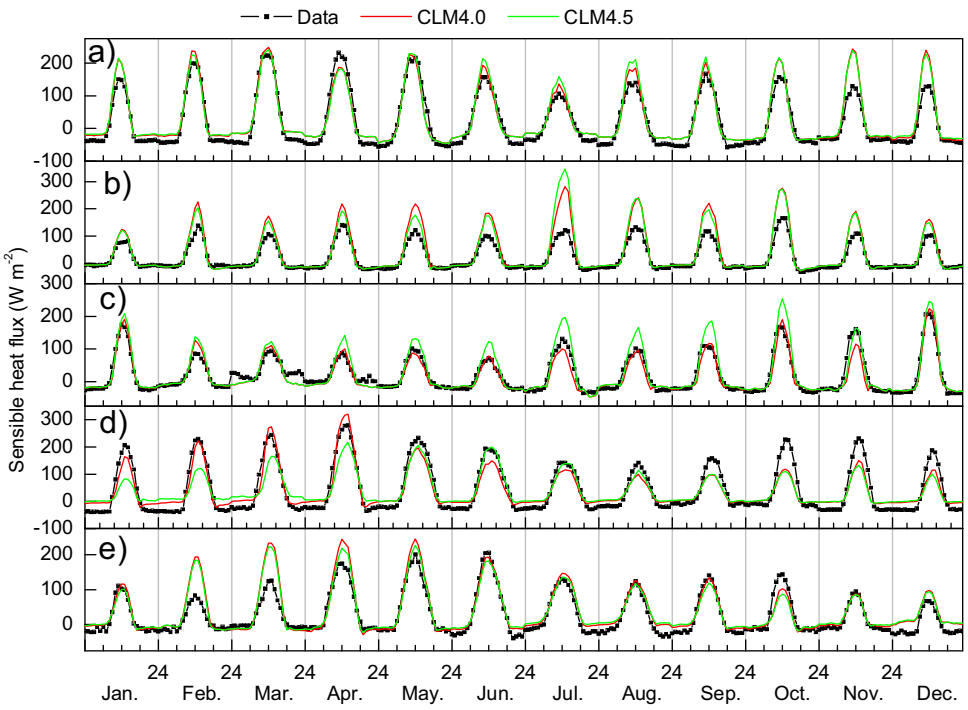

Fig. 3. Comparisons of monthly averaged diurnal variations between the models and observations at the (a) CBS, (b) QYZ, (c) DHS, (d) HBG, and (e) NMG.

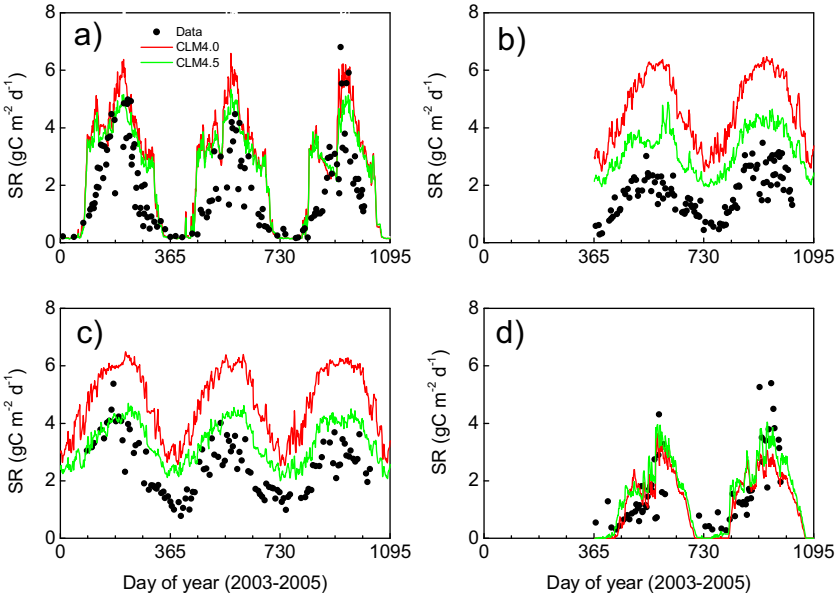

Fig. 4. Comparisons of daily soil respiration (SR) between the models and observations at (a) CBS, (b) QYZ, (c) DHS, and (d) HBG sites.

be root autotrophic respiration, accounting for 52.8%–85.9% at QYZ (Fig. 5b) and for 35.7%–56.6% at DHS (Fig. 5c). Compared to the estimated values of root respiration (171–543 g C m^{-2} yr^{-1}) observed by the trenching method (Wang, 2010) at QYZ, the high simulated root respiration (706–817 g C m^{-2} yr^{-1}) may be a major cause of the SR overestimation. The high root respiration may have resulted from overestimated root biomass for the QYZ forest, as modeled vegetation and soil carbon are consistent with observations (Zhang et al., 2010). For the DHS, the remarkable overestimation of vegetation carbon could be the main cause of RE overestimations, which are also shown via excess nighttime NEE (67%–131%) in CLM4.5 (Fig. 6h).

3.5. Temperate forest

CLM4.0 overestimates annual GPP and RE by 11% and 37% at the CBS temperate forest, resulting in an overestimated annual NEE at 271 g C m^{-2} (Figs. 2a–c). The monthly comparison shows that CLM4.0 reproduces seasonal patterns of GPP (Fig. 2f) and nighttime NEE well (Fig. 6f) but underestimates daytime carbon uptake in the summer (from June to August) by 140 g C m^{-2} (Fig. 6a). We can infer that daytime ecosystem respiration has been overestimated at CBS. By contrast, CLM4.5 significantly decreases the bias of annual RE to 12% but slightly decreases the bias of annual NEE by 4.5% due to an underestimation of annual GPP by −11% (Figs. 2a–c).

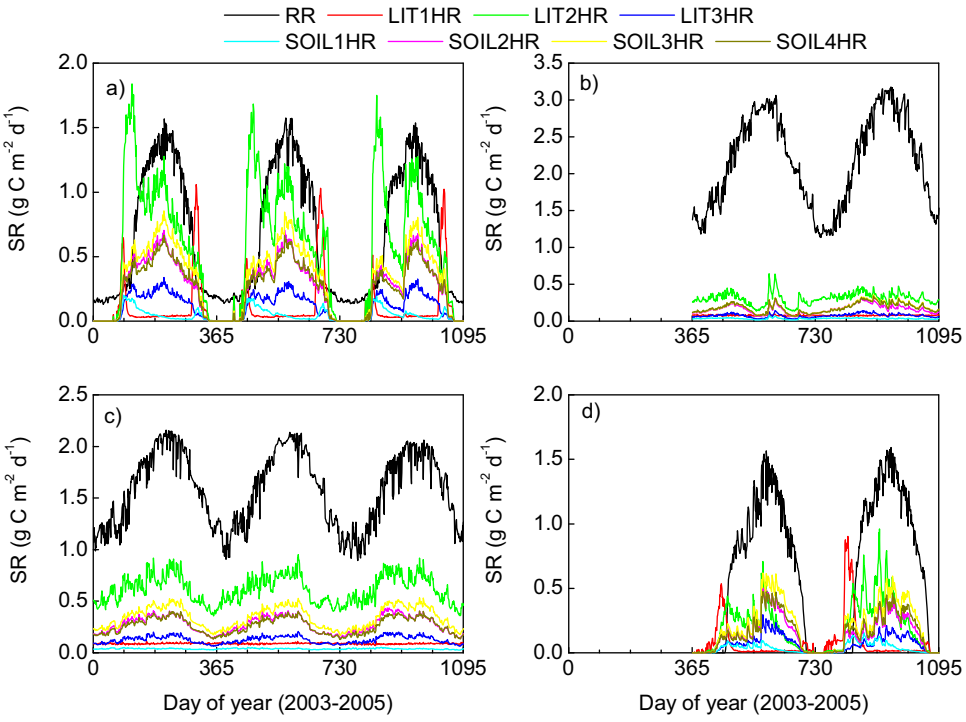

Fig. 5. Components of soil respiration modeled by CLM4.5 at the (a) CBS, (b) QYZ, (c) DHS, and (d) HBG sites. RR: root respiration; LIT1HR: heterotrophic respiration from the labile fraction of litter; LIT2HR: heterotrophic respiration from the cellulose fraction of litter; LIT3HR: heterotrophic respiration from the lignin fraction of litter; SOIL1HR: heterotrophic respiration from the soil organic matter pool at a fast decomposition rate; SOIL2HR: heterotrophic respiration from the soil organic matter pool at a moderate decomposition rate; SOIL3HR: heterotrophic respiration from the soil organic matter pool at a slow decomposition rate; SOIL4HR: heterotrophic respiration from the soil organic matter at the slowest decomposition rate.

Modifications to radiative transfer, leaf photosynthesis and stomatal conductance decrease solar radiation absorbed by vegetation and through shaded and sunlit leaf photosynthesis by −1%, −22%, and −9%, respectively. Moreover, monthly GPP was underestimated by CLM4.5, and the low bias in monthly daytime carbon uptake get worsens in the summer (Fig. 6a).

Unlike results for the two subtropical forests characterized by systematic high estimations of monthly RE for the entire year, the monthly RE bias shows a clear seasonal pattern. More specifically, excess RE mainly occurs in the spring (from March to May) and autumn (from October to November) as overestimated nighttime NEE by 123 and 63 g C m^{-2}, respectively, during the two seasons for CLM4.0 and CLM4.5 at CBS (Fig. 6f). The simulated values of daily SR are also much higher than observed values for the two seasons (Fig. 4a) as a result of large carbon release from labile and cellulose litter pools (Fig. 5a). Soil temperature overestimations at 5 cm (Fig. S4a) for the spring revealed by CLM4.0 and CLM4.5 are likely the main cause of soil respiration overestimations at CBS.

When comparing the performance of CLM4.0 and CLM4.5 at CBS, we find that CLM4.5 with the new fire model shows a remarkable underestimation of carbon fluxes and storage (Fig. 7) due to high levels of fire flux. Mean monthly GPP, NEE, vegetation carbon, soil organic carbon, and LAI modeled by CLM4.5 with the fire model active decreased by 71.1%, 46.0%, 95.3%, 88.6%, and 79.5%, respectively, compared to results derived when the fire module was turned off in the code. These results were mainly caused by an incorrect estimation of fire occurrence and thus by considerable carbon losses in the winter and spring (Fig. 7d). Fire mostly occurred when relative humidity was less than 70% and temperatures fell below zero but remained higher than −10 °C. These thresholds were globally and empirically applied to estimate the dependence of fuel combustibility on relative humidity and surface air temperatures in the fire model of CLM4.5, but they could create considerable errors, particularly over regions characterized by dry air and low temperatures and snowpack in the winter. More importantly, CLM4.5 may underestimate the value of a parameter in the fire model (i.e., the fraction of fires suppressed by humans, f_s) for forests located in national reserves with robust fire suppression capabilities, as in the case of the CBS. We modified the value of the parameter f_s to 1 and found that it could address the overestimation of fire occurrences and the incorrect underestimation of carbon storage and flux at the CBS site (Fig. 7).

3.6. Grasslands

The bias in annual NEE at the HBG alpine grassland site from 2004 to 2007 shows considerable variations, varying from −24 to 140 g C $m^{-2}yr^{-1}$ in CLM4.0 and from −54–407 g C $m^{-2}yr^{-1}$ in CLM4.5. These variations result from a dominance of variations in annual GPP over RE in driving variability. CLM4.0 and CLM4.5 show similar seasonal patterns except during June of 2007, when both daytime and nighttime NEE were strongly overestimated by CLM4.5. The high degree of carbon release modeled by CLM4.5 resulted from water stress control over deciduous phenology. The leaf area index decreased to zero from mid-May to early June (Fig. S2a), and no photosynthesis occurred thereafter due to a sustained period of water stress occurring in May (Fig. 8a), when for 15 days soil water potential accumulated above a critical threshold (−2.0 MPa) within the third model soil layer (~4.5 cm below the soil surface; Fig. S2b). The low soil water potential is likely associated with a higher LE estimation in CLM4.5 than that of the CLM4.0 (Fig. S2d). Accordingly, the decomposition of litterfall resulted in considerable carbon release in June and July of 2007 (Fig. S2c). Therefore, unreasonable simulations of water stress and phenology worsened R and RMSE for monthly NEE at HBG. Similar to results found for the temperate CBS forest, both SR and RE are overestimated at HBG

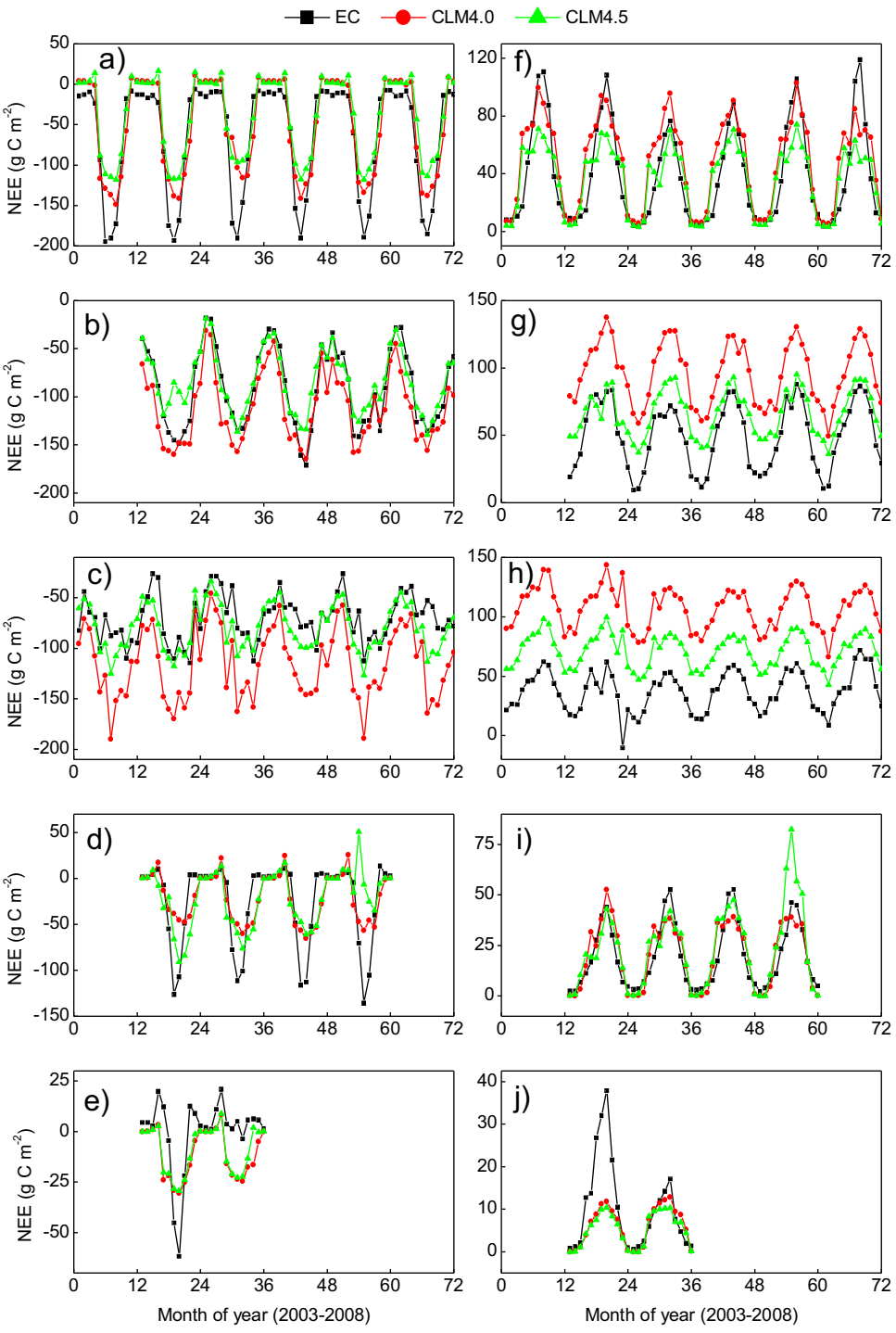

Fig. 6. Comparisons of modeled and observed daytime (a–e) and nighttime (f–j) net ecosystem exchanges of CO_2 (NEE) at CBS (a, f), QYZ (b, g), DHS (c, h), HBG (d, i), and NMG (e, j) sites.

in the spring as illustrated through daytime and nighttime monthly NEE. Higher modeled soil temperatures at 5 cm (Fig. S4g) could be associated with excess SR in the spring at HBG.

CLM4.0 and CLM4.5 perform similarly in simulating carbon fluxes at NMG grassland site. Both models underestimate annual NEE in 2004–2005 at NMG grassland site with a negative bias of 178 and 165 g C $m^{-2}yr^{-1}$ for CLM4.0 and CLM4.5 (Fig. 2e). Although the biases of annual NEE are similar between 2004 and 2005, the biases of annual GPP and RE are totally different for the two years. For CLM4.5, GPP and RE are underestimated by 26% and 58% in 2004, respectively, with abundant precipitation. In contrast, GPP is overestimated by 129% while RE is underestimated by −15% in 2005 with a lack of rainfall. CLM4.0 and CLM4.5 show marginal differences in daytime and nighttime NEE at NMG. Both models underestimate daytime NEE for the summer of 2004 with considerable rainfall but overestimate daytime NEE for 2005 and underestimate nighttime NEE for each summer. Similar to the situation at HBG with low precipitation, the modeled soil water potential for the third model soil layer was lower than −2.0 MPa from September 8–28 of 2005 (Fig. S3b). The strong water stress

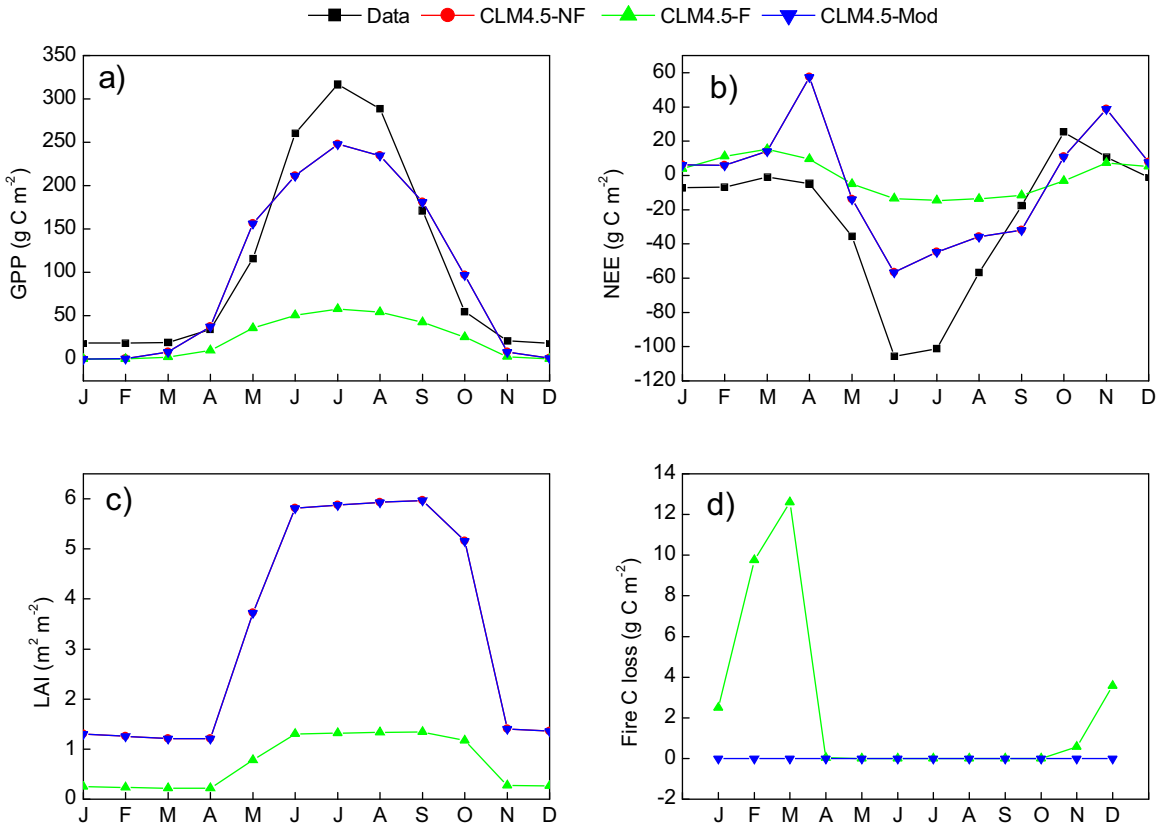

Fig. 7. Mean monthly (a) GPP, (b) NEE, (c) LAI, and (d) fire C loss at the CBS site. Data, CLM4.5-NF, CLM4.5-F, and CLM4.5-Mod represent observed values, values modeled by CLM4.5 without fire, values modeled by CLM4.5 with fire, and values modeled by CLM4.5 with changing the parameter (the fraction of fires suppressed by humans, f_s) to 1.

caused the LAI to decrease to zero by the end of September of 2005 (Fig. S3a) without photosynthesis occurring in early October of 2005 (Fig. 8b).

4. Discussion

4.1. Common issues when simulating carbon and water flux using CLM4.0 and CLM4.5

NEE is the balance of carbon uptake via canopy photosynthesis and carbon release through plant and soil respiration and disturbance. Seasonal variations of NEE are thus determined by seasonal changes in carbon assimilation and carbon release from the terrestrial ecosystem. CLM4.5 presents the same problems as CLM4.0 in simulating soil respiration in April at two deciduous sites (CBS and HBG), resulting in a considerable positive bias in the NEE. In the month of April from 2003 to 2008, modeled litter fall rates remain constant while the decomposition rate increases rapidly due to overestimated soil temperatures with increased levels of soil moisture from snow melt. High soil temperatures lead to a model overestimation of cellulose litter pool decomposition and total soil respiration. Overestimations of soil respiration for two subtropical sites (QYZ and DHS) may be primarily related to high levels of root respiration according to root respiration levels observed via the trenching method (Wang, 2010) due to the short turnover time for root litter (Todd-Brown et al., 2013). Furthermore, CLM4.0 and CLM4.5 did not capture high levels of carbon sequestration during dry seasons as revealed by eddy covariance observations at the DHS subtropical forest site (Yan, 2013a,b).

Overestimations of the length of growing season constitute another source of error in modeling seasonal NEE at deciduous forest (CBS) and grassland (HBG). CLM4.0 and CLM4.5 showed longer

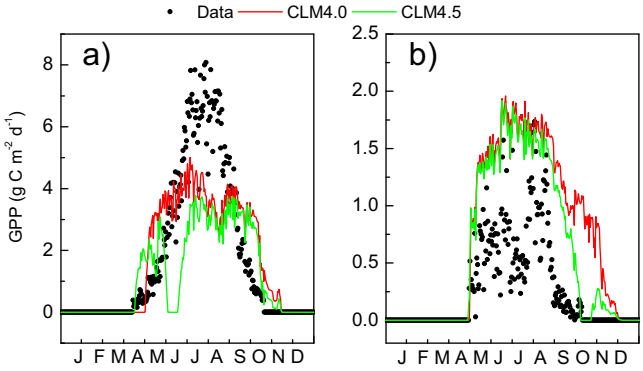

Fig. 8. Comparisons of GPP between modeled and observation result at HBG in 2007 (a) and NMG in 2005 (b).

growth periods and higher growth rates in the spring and autumn according to comparisons between the modeled GPP and estimated GPP calculated from NEE. This result is consistent with CLM4.0 GPP evaluations made using the MODIS GPP product at the global scale, which show longer GPP seasonal cycles than those observed over temperate deciduous ecosystems (Mao et al., 2012). This is a common issue facing several other state-of-the-art terrestrial biosphere models (Richardson et al., 2012).

CLM4.0 and CLM4.5 overestimate H at the three forest sites and semi-arid grassland site, especially during the daytime (Fig. 3). Differences between modeled and observed air temperatures at 2 m for the daytime reach up to 2.6° at CBS and up to 1.4° at QYZ. According to Monin-Obukhov similarity theory, H is strongly related to the difference between air and surface temperatures in the two CLM models. For vegetated surfaces, the sensible heat flux

is partitioned into vegetation and ground flux, which depend on vegetation and ground temperatures (Oleson et al., 2013). Calculations of vegetation temperatures and H from vegetation based on Newton-Raphson iterations may constitute an uncertain source and could lead to modeled canopy air temperature biases for the daytime and those for H at three forest sites. Underestimations of H for the Haibei alpine grassland site are consistent with evaluations of CLM3.5 for the same site (Lee et al., 2013).

CLM4.0 and CLM4.5 exhibit better performance in terms of seasonal patterns in latent heat flux than in terms of sensible heat flux and NEE. Latent heat flux follows a strong seasonal pattern that is well simulated by CLM4.0 and CLM4.5 with strong correlations between the model results and observations, reflecting evaluations of CLM3.5 for the Tibetan grassland site (Lee et al., 2013). Averaged RMSE ($50\,W\,m^{-2}$ for CLM4.0 and $46\,W\,m^{-2}$ for CLM4.5) levels at the five sites were lower than those ($64\,W\,m^{-2}$) estimated using five terrestrial evaporation models for 20 FLUXNET sites (Ershadi et al., 2014).

Overestimations of H and LE at the three forest sites are expected to have resulted from canopy evaporation, transpiration, and soil evaporation estimation errors. Systematic measurements on each component of evapotranspiration are essential for the further evaluation and calibration of latent heat flux estimations for vegetated surfaces. On the other hand, the energy balance is not typically closed at eddy covariance sites, though it is required to be closed in models. For example, the energy balance ratios are 0.77 and 0.82 at the QYZ and DHS sites, respectively (Li et al., 2005), and this could partially explain the apparent overestimation of energy flux by CLM.

4.2. Improvements and disadvantages of CLM4.5

CLM4.0 overestimates annual GPP and LE compared to FLUXNET-MTE for the tropics (Bonan et al., 2011). The new photosynthesis scheme used in CLM4.5 reduces the annual GPP for temperate and tropical evergreen forest by 20% and 29%, respectively, in their study. Our results show that GPP in CLM4.5 is decreased by 19% at a temperate forest site (CBS) and by 24% and 28% at two subtropical forest sites (QYZ and DHS) in comparison with the simulated GPP of the CLM4.0, supporting results reported in Bonan et al. (2011) at the global scale. Compared to estimated GPP from eddy covariance observations, annual GPP estimations were improved significantly in CLM4.5 for two subtropical sites (QYZ and DHS), where the relative error of annual GPP decreased from 51% and 107% in CLM4.0 to 15% and 50%, respectively. Phosphorus limitations at the two subtropical sites (Gao et al., 2014; Huang et al., 2013) have not been included in CLM4.5, potentially causing the model to overestimate GPP. It is necessary to examine whether GPP estimations could be improved by applying the newly developed CLM-CNP model to the phosphorus cycle (Yang et al., 2014) in the future.

Fire is an important disturbance factor that influences processes of net carbon exchange between terrestrial ecosystems and the atmosphere. Although the new process-based fire parameterization used in CLM4.5 improves the global performance of CESM (Li et al., 2013, 2012), it incorrectly estimated fire occurrence patterns for the deciduous temperate forest of the CBS examined in our study. Thresholds that were used to estimate fuel combustibility dependence on relative humidity and surface air temperatures may not be suitable for some regions. CLM4.5 may underestimate fires suppressed by humans for forests located in national reserves with robust fire suppression capabilities. The distribution map of national reserves and information on degrees of fire suppression for each national reserve are required to support modifications of this parameter at regional and global scales. Furthermore, burned areas may constitute another error source. For example, burned areas have been overestimated for some European countries and have been underestimated for years with severe fire seasons despite reductions in modeled burned area bias (Migliavacca et al., 2013).

5. Conclusions

In this study, we evaluated modifications of the new version of CLM (CLM4.5) using eddy-covariance observations of CO_2, sensible heat flux, water vapor exchange and soil respiration measurements over five ChinaFLUX tower sites, investigated the applicability of the model to different ecosystems in China, and proposed possible improvements. Our results show that CLM4.0 and CLM4.5 effectively simulated hourly NEE, H, and LE at three forest sites (0.78–0.92) with higher correlations than those at two grassland sites (0.50–0.85). Annual GPP estimations generated by CLM4.5 were improved for two subtropical forest sites as expected due to photosynthesis process modifications. However, CLM4.5 still simulates a large positive bias in subtropical GPP. NEE improvements were limited, because annual ecosystem respiration was reduced simultaneously. Moreover, these modifications increased the GPP bias for two deciduous ecosystems. CLM4.5 underestimated the annual carbon sinks of three forest sites and at one alpine grassland site while it overestimated the carbon sink of a semi-arid grassland site. This bias stems from low GPP in the summer and high respiration in the spring and autumn for deciduous ecosystems, from high respiration for subtropical forest ecosystems, and from low respiration for semi-arid grassland. Carbon sink underestimations made by CLM4.0 and CLM4.5 likely resulted from poorly simulated responses to environmental changes and disturbances, from phenological changes that are not simulated, from underestimated CO_2 fertilization effect, from underestimated N deposition trends, etc. CLM4.5 presented lower soil water content in the dry season that triggered a significant drop in LAI and GPP and a corresponding increase in respiration at two grassland sites. Given its potentially strong effect on the seasonal cycle of carbon flux, more attention should be given to better understanding drought deciduous phenology patterns in CLM. Comparisons made between remote sensing LAI datasets may help identify possible seasonal drought-driven phenology errors in the absence of eddy covariance flux measurements. Both CLM4.5 and CLM4.0 better simulated latent heat flux than sensible heat flux. Poorer performance results found in terms of monthly sensible heat flux may be due to overpredicted sensible heat exchanges from vegetation. The new fire parameterization used in CLM4.5 caused excessive, unrealistic fire estimations during the cold season at the Changbaishan forest site that resulted in unexpected underestimations of carbon flux and storage. The fire model should be switched off for site level comparisons, or the fire parameter may require local adjustments for regions characterized by cold and dry winters and by high levels of human suppression. Continued improvements made to CLM will require better estimations of seasonal GPP and respiration influenced by seasonal water conditions, sensible heat exchange from vegetation, and the partitioning of net radiation between sensible and heat flux.

Acknowledgments

This work was financially supported by the National Key Research and development program of China (2015CB954102), the National Natural Science Foundation of China (31290221, 31420103917), and the Strategic Priority Research Program of the Chinese Academy of Sciences (XDA05050602). We thank all related staff from ChinaFLUX and CERN for their contributions from observations to data processing. This research was supported in part by the US Department of Energy (DOE), Office of Science, Biological

and Environmental Research. The Oak Ridge National Laboratory is managed by UT-BATTELLE for DOE under contract DE-AC05-00OR22725.

Appendix A. Supplementary data

Supplementary data associated with this article can be found, in the online version, at http://dx.doi.org/10.1016/j.agrformet.2016.05.018.

References

Balzarolo, M., et al., 2014. Evaluating the potential of large-scale simulations to predict carbon fluxes of terrestrial ecosystems over a european eddy covariance network. Biogeosciences 11 (10), 2661–2678.

Boisserie, M., Shin, D.W., Larow, T.E., Cocke, S., 2006. Evaluation of soil moisture in the Florida state university climate model—National Center for Atmospheric Research community land model (FSU-CLM) using two reanalyses (R2 and ERA40) and in situ observations. J. Geophys. Res.-Atmos. 111, D08103.

Bonan, G.B., et al., 2011. Improving canopy processes in the community land model version 4 (CLM4) using global flux fields empirically inferred from FLUXNET data. J. Geophys. Res.-Biogeosci. 116, G02014.

Bonan, G.B., Oleson, K.W., Fisher, R.A., Lasslop, G., Reichstein, M., 2012. Reconciling leaf physiological traits and canopy flux data: use of the TRY and FLUXNET databases in the community land model version 4. J. Geophys. Res.-Biogeosci. 117, G02026.

Bonan, G.B., 2014. Connecting mathematical ecosystems, real-world ecosystems, and climate science. New Phytol. 202 (3), 731–733.

Cramer, W., et al., 2001. Global response of terrestrial ecosystem structure and function to CO2 and climate change: results from six dynamic global vegetation models. Glob. Change Biol. 7 (4), 357–373.

De Kauwe, M.G., et al., 2013. Forest water use and water use efficiency at elevated CO2: a model-data intercomparison at two contrasting temperate forest FACE sites. Glob. Change Biol. 19 (6), 1759–1779.

De Kauwe, M.G., et al., 2014. Where does the carbon go? A model-data intercomparison of vegetation carbon allocation and turnover processes at two temperate forest free-air CO enrichment sites. New Phytol. 203 (3), 883–899.

Ershadi, A., McCabe, M.F., Evans, J.P., Chaney, N.W., Wood, E.F., 2014. Multi-site evaluation of terrestrial evaporation models using FLUXNET data. Agric. For. Meteorol. 187, 46–61.

Falge, E., et al., 2001. Gap filling strategies for defensible annual sums of net ecosystem exchange. Agric. For. Meteorol. 107 (1), 43–69.

Forster, P.M., et al., 2013. Evaluating adjusted forcing and model spread for historical and future scenarios in the CMIP5 generation of climate models. J. Geophys. Res.-Atmos. 118 (3), 1139–1150.

Friedlingstein, P., Dufresne, J.L., Cox, P.M., Rayner, P., 2003. How positive is the feedback between climate change and the carbon cycle? Tellus Ser. B-Chem. Phys. Meteorol. 55 (2), 692–700.

Friedlingstein, P., et al., 2014. Uncertainties in CMIP5 climate projections due to carbon cycle feedbacks. J. Clim. 27 (2), 511–526.

Fu, Y.L., Yu, G.R., Wang, Y.F., Li, Z.Q., Hao, Y.B., 2006. Effect of water stress on ecosystem photosynthesis and respiration of a leymus chinensis steppe in Inner Mongolia. Sci. China Ser. D-Earth Sci. 49, 196–206.

Gao, Y., He, N.P., Yu, G.R., Chen, W.L., Wang, Q.F., 2014. Long-term effects of different land use types on C, N, and P stoichiometry and storage in subtropical ecosystems: a case study in China. Ecol. Eng. 67, 171–181.

Hao, Y.B., et al., 2006. Seasonal variation in carbon exchange and its ecological analysis over leymus chinensis steppe in Inner Mongolia. Sci. China Ser. D-Earth Sci. 49, 186–195.

He, M.Z., et al., 2013. Evaluation and improvement of MODIS gross primary productivity in typical forest ecosystems of East Asia based on eddy covariance measurements. J. For. Res.-Jpn. 18 (1), 31–40.

He, H.L., et al., 2014. Large-scale estimation and uncertainty analysis of gross primary production in Tibetan alpine grasslands. J. Geophys. Res.-Biogeosci. 119 (3), 466–486.

Hu, Z.M., et al., 2008. Effects of vegetation control on ecosystem water use efficiency within and among four grassland ecosystems in China. Glob. Change Biol. 14 (7), 1609–1619.

Huang, M., et al., 2007. The ecosystem carbon accumulation after conversion of grasslands to pine plantations in subtropical red soil of South China. Tellus Ser. B-Chem. Phys. Meteorol. 59 (3), 439–448.

Huang, W.J., et al., 2013. Increasing phosphorus limitation along three successional forests in Southern China. Plant Soil 364 (1–2), 181–191.

Huntzinger, D.N., et al., 2012. North american carbon program (NACP) regional interim synthesis: terrestrial biospheric model intercomparison. Ecol. Modell. 232, 144–157.

Ichii, K., et al., 2013. Site-level model-data synthesis of terrestrial carbon fluxes in the CarboEastAsia eddy-covariance observation network: toward future modeling efforts. J. For. Res.-Jpn. 18 (1), 13–20.

Ju, W., Wang, S., Yu, G., Zhou, Y., Wang, H., 2010. Modeling the impact of drought on canopy carbon and water fluxes for a subtropical evergreen coniferous plantation in Southern China through parameter optimization using an ensemble Kalman filter. Biogeosciences 7 (3), 845–857.

Jung, M., et al., 2007a. Assessing the ability of three land ecosystem models to simulate gross carbon uptake of forests from boreal to Mediterranean climate in Europe. Biogeosciences 4 (4), 647–656.

Jung, M., et al., 2007b. Uncertainties of modeling gross primary productivity over Europe: a systematic study on the effects of using different drivers and terrestrial biosphere models. Glob. Biogeochem. Cycles 21 (4), GB4021.

Koven, C.D., et al., 2013. The effect of vertically resolved soil biogeochemistry and alternate soil C and N models on C dynamics of CLM4. Biogeosciences 10 (11), 7109–7131.

Kim, Y., Wang, G.L., 2005. Modeling seasonal vegetation variation and its validation against moderate resolution imaging spectroradiometer (MODIS) observations over north america (vol 110, art no D04106, 2005). J. Geophys. Res.-Atmos. 110, D07104.

Lawrence, P.J., Chase, T.N., 2007. Representing a new MODIS consistent land surface in the community land model (CLM 3.0). J. Geophys. Res.-Biogeosci. 112, G01023.

Lawrence, D.M., et al., 2011. Parameterization improvements and functional and structural advances in version 4 of the community land model. J. Adv. Model. Earth Syst. 3, M03001.

Lee, Y.H., Lim, H.J., Ichii, K., Li, Y.N., 2013. Evaluation of the Community Land Model 3.5 with carbon and nitrogen cycles (CLM3.5CN) at a Tibetan grassland site. Asia-Pac. J. Atmos. Sci. 49 (5), 561–570.

Li, Z.Q., et al., 2005. Energy balance closure at ChinaFLUX sites. Sci. China Ser. D-Earth Sci. 48, 51–62.

Li, H.Y., et al., 2011. Evaluating runoff simulations from the Community Land Model 4.0 using observations from flux towers and a mountainous watershed. J. Geophys. Res.-Atmos. 116, D24120.

Li, F., Zeng, X.D., Levis, S., 2012. A process-based fire parameterization of intermediate complexity in a dynamic global vegetation model. Biogeosciences 9 (7), 2761–2780.

Li, F., Levis, S., Ward, D.S., 2013. Quantifying the role of fire in the earth system—Part 1: improved global fire modeling in the Community Earth System Model (CESM1). Biogeosciences 10 (4), 2293–2314.

Mao, J.F., Thornton, P.E., Shi, X.Y., Zhao, M.S., Post, W.M., 2012. Remote sensing evaluation of CLM4 GPP for the period 2000-09. J. Clim. 25 (15), 5327–5342.

Mao, J.F., et al., 2015. Disentangling climatic and anthropogenic controls on global terrestrial evapotranspiration trends. Environ. Res. Lett. 10 (9), 094008.

Migliavacca, M., et al., 2013. Modeling burned area in europe with the community land model. J. Geophys. Res.-Biogeosci. 118 (1), 265–279.

Morales, P., et al., 2005. Comparing and evaluating process-based ecosystem model predictions of carbon and water fluxes in major European forest biomes. Glob. Change Biol. 11 (12), 2211–2233.

Niu, G.Y., Yang, Z.L., 2007. An observation-based formulation of snow cover fraction and its evaluation over large North American river basins. J. Geophys. Res.-Atmos. 112, D21101.

Niu, G.Y., Yang, Z.L., Dickinson, R.E., Gulden, L.E., 2005. A simple TOPMODEL-based runoff parameterization (SIMTOP) for use in global climate models. J. Geophys. Res.-Atmos. 110, D21106.

Oleson, K.W., Lawrence, D.M., Bonan, G.B., Drewniak, B., Huang, M., Koven, C.D., Levis, S., Li, F., Riley, W.J., Subin, Z.M., Swenson, S.C., Thornton, P.E., Bozbiyik, A., Fisher, R., Kluzek, E., Lamarque, J.-F., Lawrence, P.J., Leung, L.R., Lipscomb, W., Muszala, S., Ricciuto, D.M., Sacks, W., Sun, Y., Tang, J., Yang, Z.-L., 2013. Technical Description of Version 4.5 of the Community Land Model (CLM). Ncar Technical Note NCAR/TN-503 + STR. National Center for Atmospheric Research, Boulder, pp. 422.

PaiMazumder, D., et al., 2008. Evaluation of community climate system model soil temperatures using observations from Russia. Theor. Appl. Climatol. 94 (3–4), 187–213.

Piao, S.L., et al., 2011. Contribution of climate change and rising CO2 to terrestrial carbon balance in East Asia: a multi-model analysis. Glob. Planet. Change 75 (3–4), 133–142.

Piao, S., et al., 2013. Evaluation of terrestrial carbon cycle models for their response to climate variability and to CO_2 trends. Glob. Change Biol. 19 (7), 2117–2132.

Qian, T.T., Dai, A., Trenberth, K.E., Oleson, K.W., 2006. Simulation of global land surface conditions from 1948 to 2004. Part I: forcing data and evaluations. J. Hydrometeorol. 7 (5), 953–975.

Raczka, B.M., et al., 2013. Evaluation of continental carbon cycle simulations with North American flux tower observations. Ecol. Monogr. 83 (4), 531–556.

Ren, X.L., et al., 2013. Uncertainty analysis of modeled carbon and water fluxes in a subtropical coniferous plantation. J. Geophys. Res.-Biogeosci. 118 (4), 1674–1688.

Richardson, A.D., et al., 2012. Terrestrial biosphere models need better representation of vegetation phenology: results from the North American carbon program site synthesis. Glob. Change Biol. 18 (2), 566–584.

Schaefer, K., et al., 2012. A model-data comparison of gross primary productivity: results from the North American carbon program site synthesis. J. Geophys. Res.-Biogeosci. 117, G03010.

Schwalm, C.R., et al., 2010. A model-data intercomparison of CO2 exchange across north america: results from the north american carbon program site synthesis. J. Geophys. Res.-Biogeosci. 115, G00H05.

Shi, X.Y., Mao, J.F., Thornton, P.E., Hoffman, F.M., Post, W.M., 2011. The impact of climate CO2, nitrogen deposition and land use change on simulated contemporary global river flow. Geophys. Res. Lett. 38, L08704.

Shi, X.Y., Mao, J.F., Thornton, P.E., Huang, M.Y., 2013. Spatiotemporal patterns of evapotranspiration in response to multiple environmental factors simulated by the community land model. Environ. Res. Lett. 8 (2), 024012.
Sitch, S., et al., 2008. Evaluation of the terrestrial carbon cycle, future plant geography and climate-carbon cycle feedbacks using five Dynamic Global Vegetation Models (DGVMs). Glob. Change Biol. 14 (9), 2015–2039.
Stockli, R., et al., 2008. Use of FLUXNET in the community land model development. J. Geophys. Res.-Biogeosci. 113, G01025.
Sun, Y., Gu, L.H., Dickinson, R.E., 2012. A numerical issue in calculating the coupled carbon and water fluxes in a climate model. J. Geophys. Res. Atmos. 117, D22103.
Swenson, S.C., Lawrence, D.M., Lee, H., 2012. Improved simulation of the terrestrial hydrological cycle in permafrost regions by the community land model. J. Adv. Model. Earth Syst. 4, M08002.
Tang, Y.K., Wen, X.F., Sun, X.M., Wang, H.M., 2014. Interannual variation of the bowen ratio in a subtropical coniferous plantation in southeast China, 2003–2012. PLoS One 9 (2), e88267.
Tao, B., et al., 2007. Spatial patterns of terrestrial net ecosystem productivity in China during 1981–2000. Sci. China Ser. D-Earth Sci. 50 (5), 745–753.
Thomas, R.Q., Zaehle, S., Templer, P.H., Goodale, C.L., 2013. Global patterns of nitrogen limitation: confronting two global biogeochemical models with observations. Glob. Change Biol. 19 (10), 2986–2998.
Thornton, P.E., Lamarque, J.F., Rosenbloom, N.A., Mahowald, N.M., 2007. Influence of carbon-nitrogen cycle coupling on land model response to CO2 fertilization and climate variability. Glob. Biogeochem. Cycles 21 (4), GB4018.
Thornton, P.E., et al., 2009. Carbon-nitrogen interactions regulate climate-carbon cycle feedbacks: results from an atmosphere-ocean general circulation model. Biogeosciences 6 (10), 2099–2120.
Todd-Brown, K.E.O., et al., 2013. Causes of variation in soil carbon simulations from CMIP5 earth system models and comparison with observations. Biogeosciences 10 (3), 1717–1736.
Walker, A.P., et al., 2014. Comprehensive ecosystem model-data synthesis using multiple data sets at two temperate forest free-air CO2 enrichment experiments: model performance at ambient CO2 concentration. J. Geophys. Res.: Biogeosci. 119 (5), 937–964.
Wang, Z., et al., 2004. Using MODIS BRDF and albedo data to evaluate global model land surface albedo. J. Hydrometeorol. 5 (1), 3–14.
Wang, A., Li, K.Y., Lettenmaier, D.P., 2008. Integration of the variable infiltration capacity model soil hydrology scheme into the community land model. J. Geophys. Res.-Atmos. 113, D09111.
Wang, Y., 2010. Soil Respiration and Its Response Mechanism to Environment of Different Forest Types in Subtropical China. Chinese Academy of Sciences, Beijing.
Wenzel, S., et al., 2014. Emergent constraints on climate-carbon cycle feedbacks in the CMIP5 earth system models. J. Geophys. Res.: Biogeosci. 119 (5), 794–807.
Yan, H.M., et al., 2009. Modeling gross primary productivity for winter wheat-maize double cropping system using MODIS time series and CO2 eddy flux tower data. Agric. Ecosyst. Environ. 129 (4), 391–400.
Yan, J.H., et al., 2013a. Substantial amounts of carbon are sequestered during dry periods in an old-growth subtropical forest in South China. J. For. Res.-Jpn. 18 (1), 21–30.
Yan, J.H., et al., 2013b. Seasonal and inter-annual variations in net ecosystem exchange of two old-growth forests in Southern China. Agric. For. Meteorol. 182, 257–265.
Yang, X., Thornton, P.E., Ricciuto, D.M., Post, W.M., 2014. The role of phosphorus dynamics in tropical forests—a modeling study using CLM-CNP. Biogeosciences 11 (6), 1667–1681.
Yu, G.R., et al., 2006. Overview of ChinaFLUX and evaluation of its eddy covariance measurement. Agric. For. Meteorol. 137 (3–4), 125–137.
Yu, G.R., et al., 2008. Water-use efficiency of forest ecosystems in Eastern China and its relations to climatic variables. New Phytol. 177 (4), 927–937.
Yu, G.R., et al., 2014. High carbon dioxide uptake by subtropical forest ecosystems in the East Asian monsoon region. Proc. Natl. Acad. Sci. U. S. A. 111 (13), 4910–4915.
Zaehle, S., et al., 2014. Evaluation of 11 terrestrial carbon-nitrogen cycle models against observations from two temperate free-air CO2 enrichment studies. New Phytol. 202 (3), 803–822.
Zhang, D.Q., et al., 2006a. Seasonal dynamics of soil CO2 effluxes with responses to environmental factors in lower subtropical forests of China. Sci. China Ser. D-Earth Sci. 49, 139–149.
Zhang, L.M., et al., 2006b. Seasonal variation of carbon exchange of typical forest ecosystems along the eastern forest transect in China. Sci. China Ser. D-Earth Sci. 49, 47–62.
Zhang, L., Luo, Y.Q., Yu, G.R., Zhang, L.M., 2010. Estimated carbon residence times in three forest ecosystems of Eastern China: applications of probabilistic inversion. J. Geophys. Res.-Biogeosci. 115, G01010.
Zhao, L., et al., 2006. Diurnal, seasonal and annual variation in net ecosystem CO2 exchange of an alpine shrubland on Qinghai-Tibetan plateau. Glob. Change Biol. 12 (10), 1940–1953.
Zheng, Z.M., et al., 2009. Temperature sensitivity of soil respiration is affected by prevailing climatic conditions and soil organic carbon content: a trans-China based case study. Soil Biol. Biochem. 41 (7), 1531–1540.